Characterization of Folded Conformations in a Tetrapeptide Containing Two Tryptophan Residues by Vibrational Circular Dichroism

ANA G. PETROVIC,[1] PRASAD L. POLAVARAPU,[1]* R. MAHALAKSHMI,[2] AND P. BALARAM[2]*
[1]*Department of Chemistry, Vanderbilt University, Nashville, Tennessee*
[2]*Molecular Biophysics Unit, Indian Institute of Science, Bangalore, India*

Contribution to the special thematic project "Advances in Chiroptical Methods"

ABSTRACT The intramolecularly hydrogen bonded conformations of the tetrapeptide Boc-Trp-Aib-Gly-Trp-OMe (WUGW) are investigated using experimental and quantum chemical predictions of vibrational circular dichroism (VCD) in the 1800–1550 cm^{-1} region. The predicted VCD spectrum, for a conformation (conformer A) obtained from optimization of crystal structure, reproduced the dominant negative VCD band observed experimentally in CH_3OH and $CHCl_3$ solvents. However, the predicted VCD spectrum of Conformation A also has an extra positive band which is not seen in the experimental spectra. This mismatch appears to be due to the lack of solvent influence in the quantum chemical geometry optimizations. However, Conformations I and II, obtained, respectively, from constrained optimization of crystal and NMR structures, mimic the solvent stabilized structures and are predicted to have dominant negative VCD band as found in the experimental spectra. It is noted that, for the peptide investigated here, unconstrained quantum chemical geometry optimizations in vacuum converged to structures that are not the realistic models of conformations found in solution. It is also noted that undertaking quantum chemical vibrational property calculations directly using geometries obtained from crystal data or NMR data resulted in unrealistic vibrational frequencies and descriptions. However, constraining the backbone dihedral angles to those found in condensed medium, and optimizing the remaining geometrical parameters resulted in a better reproduction of the observed VCD in condensed medium. The vibrational origins of bands in all of the predicted VCD spectra for the WUGW-tetrapeptide have also been presented. *Chirality 21:S76–S85, 2009.* © 2009 Wiley-Liss, Inc.

KEY WORDS: tetrapeptide; WUGW peptide; beta turns; infrared absorption; vibrational circular dichroism; density functional predictions

INTRODUCTION

Structures of biomolecules are typically investigated using X-ray crystallography, nuclear magnetic resonance (NMR), and/or electronic circular dichroism (ECD), depending on the applicability of these individual methods. Recently, vibrational circular dichroism (VCD) spectroscopy has emerged as a powerful method for the structural elucidation of peptides and proteins in solution and film states. Although both ECD and VCD spectroscopies allow investigation of peptide and protein structures, the ECD spectral interpretations are sometimes ambiguous[1–3] when aromatic residues are present. This is because aromatic amino acids (Phe, Tyr, Trp) have electronic transitions in the far UV-region (190–230 nm) that overlap[1] with those of amide groups and, as a consequence, ECD associated with these transitions can interfere with each other. On the other hand, as the vibrational transitions of aromatic residues and amide groups are well separated in frequency positions, VCD associated with these transitions do not interfere with each other. Thus, VCD spectroscopy offers definite advantages for structural determination of peptides and proteins that contain aromatic residues. The tetrapeptide investigated here contains two aromatic residues.

A number of studies[4–19] have used VCD spectroscopy to derive conformationally sensitive information for protein/peptide systems. The secondary structures are reflected in the recognizable VCD signatures associated with the amide I (C=O stretch) and amide II (N—H deformation)

© 2009 Wiley-Liss, Inc.

Contract grant sponsor: National Center for Supercomputing Applications; Contract grant numbers: #CHE060063T, #CHE090061.
Present address for R. Mahalakshmi is Indian Institute of Science Education and Research, Bhopal, India.
*Correspondence to: Prasad L. Polavarapu, Department of Chemistry, Vanderbilt University, Nashville, TN 37235, USA. E-mail: prasad.l.polavarapu@vanderbilt.edu and P. Balaram, Molecular Biophysics Unit, Indian Institute of Science, Bangalore 560012, India. E-mail: pb@mbu.iisc.ernet.in
Received for publication 7 May 2009; Accepted 17 July 2009
DOI: 10.1002/chir.20779
Published online 11 September 2009 in Wiley InterScience (www.interscience.wiley.com).

vibrations. Although a majority of structural elucidations of peptides/proteins using VCD spectroscopy have been accomplished with empirical spectra-structure correlations, some predictive calculations have also been attempted. Initial VCD predictions[1,20] have been based on extended coupled oscillator model,[21] which assumes[22] dipole–dipole coupling between amide groups of amino acid units as the source of the optical activity. Keiderling and coworkers have promoted[23–31] correlations of the experimental VCD spectra with corresponding approximate quantum chemical spectra using a transfer parameter method. This method relies on transferring parameters (geometry, force constants, and atomic tensors) obtained for smaller peptides, typically di- or tri-peptides, to larger polypeptides or proteins. This approach was deemed to give satisfactory predicted-experimental spectral correlations, while avoiding the high computational cost of fully quantum chemical treatment for larger systems. This method has been implemented for α-helical,[25,26] β-sheet,[27,28] and β-hairpin[29–31] secondary structures. However, the transfer method does not address or verify fundamental rules such as the sum rules for force constants[32] and atomic tensors[33–35] following the transfer of these parameters. As a result it is not clear whether, or not, the transfer parameter method gives satisfactory predicted-experimental spectral correlations for the "right" reasons. Furthermore, for aromatic systems, such as the one considered here, the π–π interactions between aromatic residues can dominate and such interactions are not likely to be represented correctly in the transfer parameter method.

Quantum chemical optimizations and VCD predictions, without transferring parameters, have been performed on alanine-based decaamide,[36,37] with helical secondary structure, and alanine-based triamide[38] with β-sheet arrangement. Such fully quantum chemical VCD predictions have not been undertaken for hetero-amino-acid peptides or peptides capable of forming β-hairpin and β-turn type structures. In the case of cyclosporin, a 11-member cyclic peptide containing β-turn and sheet structural components, quantum chemical predictions of VCD obtained for fragment models[39] were used to interpret the experimental VCD spectra.

Among the secondary structures of peptides and proteins, turn geometry displays[40–43] considerable conformational variability. Turn is the non-repeating area where a polypeptide chain reverses its overall direction. In β-turn, this area comprises four amino acid residues, while in γ-turns three residues. Beside β- and γ-turns, additional types of turns are also known to exist.[40–43] If four residues comprising a β-turn are labeled consecutively as i, $i+1$, $i+2$, and $i+3$ then the values of φ_{i+1}, ψ_{i+1}, φ_{i+2}, ψ_{i+2} angles define[41–43] the type of β-turn. These angles, respectively, of -60°, -30°, -90°, and 0° define Type I, -60°, 120°, 80°, and 0° define Type II, and -60°, -30°, -60°, and -30° define Type III. The corresponding angles with opposite signs define prime turns, Type I′, II′, and III′, respectively (which are also called inverse turns). β-hairpins usually contain[41] Type I′ or II′ β-turns. Unlike fairly well-established VCD signatures for α-helix, β-sheet, and random-coil secondary structures,[23,44] characteristic VCD features for peptides exhibiting a turn motif have not been well defined. Xie et al. have reported[20] based on both experimental and theoretical considerations that cyclic-peptides display a positive couplet in the amide I region as a dominant signature of Type I or Type II β-turns. Specifically, Type I turn was associated with the couplet at $\sim$1675/1690 cm^{-1}, while Type II turn was associated with a broader couplet at $\sim$1635/1690 cm^{-1}. However, the positive VCD couplet in the amide I region can also be interpreted[45] as indicative of a γ-turn for cyclic-peptides. A different study,[46] performed by Wyssbrod et al., has suggested that for cyclic-peptides with at least four residues, β-turn characterizing VCD pattern in the amide I region is a negative-positive-negative signal. Experimentally and theoretically considered VCD spectra for turn-forming tetrapeptides, reported[47] by Hilario et al., have displayed a negative VCD couplet in amide I region. It was also indicated in the literature[46] that linear hexapeptides exhibit amide I VCD pattern that is more complex than just a single couplet. On the basis of the previous VCD studies,[20,45–48] there is no prototypical VCD signature for turn as a secondary structural motif. VCD spectra may be able to distinguish among various types of turn conformations, but to establish conformational details of these turn conformations it is necessary to simultaneously obtain and compare the experimental and theoretical VCD spectra for peptides that have propensity for turn conformations.

β-hairpin structures result from a mixture of β-sheet and turn motifs. β-hairpins generally yield[1,2] an intense negative VCD band in the $\sim$1645 cm^{-1} region and sometimes also a weak positive VCD band at $\sim$1690 cm^{-1}. Parallel β-sheet structures typically give[4–19] one negative VCD signal at about $\sim$1630 cm^{-1}. If both β-sheet and hairpin structures yield negative VCD signals then turn structure may also be associated with a negative VCD signal or no VCD signal at all. But to establish the VCD signature of turn motifs it is necessary to investigate the peptides that have turn structure only and no other secondary structural motif.

Although quantum chemical VCD simulations for β-turn-forming tetrapeptides have been considered in the past,[47] the tetrapeptides for which these simulations have been performed differ in residue-composition from the tetrapeptide used for experimental investigation. Specifically, experimentally investigated tetrapeptides were Ac-Val-Asn-Gly-Lys-NH_2 and Ac-Val-Pro-Gly-Lys-NH_2, while theoretical investigation were conducted for tetra peptides with all residues, other than Pro and Gly, substituted with Ala residue. The geometry used for the calculations on these β-turn models is not a quantum chemically optimized geometry, but a Type I′ turn geometry extracted from the NMR structure of a larger peptide.

More recently, Keiderling and coworkers[49] have reported a modeling study to establish the expected VCD signatures for Type I, I′, II, II′, III, and III′ β turns using Ac-Aib-Gly-NMe, Ac-Ala-Ala-NMe, and Ac-^{D}Pro-Gly-NMe as model compounds. However, experimental data are not

available for these model compounds to assess the validity of predictions obtained.

From the literature background provided in the previous paragraphs, two deficiencies are apparent: (a) experimental VCD spectra for a short peptide with β-turn as the sole structural motif are not available; (b) Fully quantum chemical predictions of VCD spectra for the same β-turn-forming peptide, as the one experimentally studied, have not been reported to date. These deficiencies are remedied in the current study by presenting the first combined experimental and quantum chemical investigation, including both geometry optimization and VCD spectral prediction, done on the entire tetrapeptide that is residue-for-residue equivalent to the tetrapeptide investigated experimentally.

The tetrapeptide under investigation is Boc-Trp_1-Aib_2-Gly_3-Trp_4-OMe (WUGW)[50] and it falls under the class of small tetrapeptides that exhibit well defined folded structures. This sequence (WUGW) was chosen to examine the folding propensity of the Aib-Gly segment when flanked by bulky aromatic Trp residues. The Aib-Gly segment has been previously shown to have strong tendency to form β turn conformations with two residues occupying the (i+1) and (i+2) positions. The choice of the present sequence was intended to examine the role of aromatic interactions across the i and (i+3) positions. Earlier studies from this laboratory have examined aromatic interactions in both the helices[51] and hairpins.[52] The achiral nature of the Aib and Gly residues permits the central β turn to adopt either a Type I/III or Type I′/III′ β turn conformation. The prime turns facilitate registered anti-parallel hairpin conformations while Type I/III turns can nucleate helical folding.[53,54] For the current WUGW-tetrapeptide, X-ray and NMR studies[50] establish the presence of folded β-turn conformation. ECD spectrum of this tetrapeptide in CH_3OH is anomalous and direct interpretation of secondary structure was not possible[50] from that spectrum. The reported[50] X-ray and NMR studies on this tetrapeptide suggest the presence of folded reverse turn conformations. The quantum chemical predictions of stable conformations, and of conformation dependent VCD spectra, along with the vibrational origins of the dominant VCD signals, would be of significant importance for this tetrapeptide. The comparison of predicted VCD spectra for different conformers with the experimental VCD spectra for this tetrapeptide may permit identification of the characteristic VCD signatures for some of the turn-alone type structures.

EXPERIMENTAL

The vibrational absorption (VA) and VCD spectra were recorded in the 2000–900 cm^{-1} region using a commercial Fourier transform VCD spectrometer modified[55] to reduce the level of artifacts. The VCD spectra were recorded with 3 h data collection time at 4 cm^{-1} resolution. The sample was held in demountable cell with CaF_2 windows and a 100 μm spacer. Spectra were measured in $CHCl_3$ and CH_3OH solvents at a concentration of ~2 mg in 100 μl. Baseline corrections for all spectra were made by subtracting the absorption (or VCD) of the corresponding solvent. Spectral region below ~1550 cm^{-1} has been omitted due to the interference from the solvent absorption.

The quantum chemical calculations were done using Gaussian 03 program. Theoretical optimizations and VA and VCD predictions were done using B3LYP functional and 6-31G* basis set. Other functionals and larger basis sets were not explored due to the constraints of computing time. Lorentzian band shapes, with a bandwidth of 10 cm^{-1}, were used for spectral simulation. Predicted frequencies associated with optimized conformations A and B and constraints-imposed partially optimized Conformations I and II have been scaled by a factor of 0.9613.

RESULTS AND DISCUSSION

The WUGW-tetrapeptide provides a good model for studying multiple well folded conformations in a short peptide. The central Aib-Gly segment is capable of adopting both Type I and I′ structures. The flanking Trp residues can influence conformational choice by aromatic-amide interactions. The crystal structure of the WUGW peptide establishes a consecutive β-turn conformation, while NMR results provided evidence for interconversion between two conformers with equal populations in solution, one of which is also observed in the X-ray analysis.[50] In this report, we investigate the secondary structure of WUGW-tetrapeptide using combined experimentally observed and quantum chemically predicted VCD spectra.

The geometry optimization of WUGW peptide involved consideration of three starting structures (Conformations I–III as given in Fig. 1). Each of the three starting structures represents a folded, fairly compact conformation with two hydrogen bonds. Conformation I is based on the coordinates obtained from an X-ray diffraction study[50] of WUGW peptide crystals. This initial conformation exhibits backbone folding and is classified as a consecutive Type II–I′ β-turn.[50] Conformation II is one of the conformations suggested by the NMR resuts[50] and its dihedral angles resemble the conventional Type I′ β-turn at the Aib-Gly segment. These two initial conformations are representatives of β-turn secondary structures and differ only in the φ dihedral angle of Trp_1 residue (refer Table 1): this angle is ~−55° for Conformation I and ~−150° for Conformation II. Conformation III has been constructed to model a 3_{10}-helical structure, which is widely observed in Aib containing peptides.[56–59] The main structural parameters of these three initial conformations are presented in Table 1. These parameters include standard backbone dihedral angles (φ, ψ, ω) associated with each of the four amino acids and dihedral angles (χ_1, χ_2) associated with the orientation of two Trp residues.

The intra-molecular hydrogen bonds are depicted in Figure 1. For Conformation I, one hydrogen bond (~2.29 Å) is between Trp_1 C=O and Trp_4 N—H, and another hydrogen bond (~1.85 Å) is between Boc-ester C=O and Gly_3 N—H. For Conformation II, one hydrogen bond (~2.29 Å) is between Trp_1 C=O and Trp_4 N—H, and

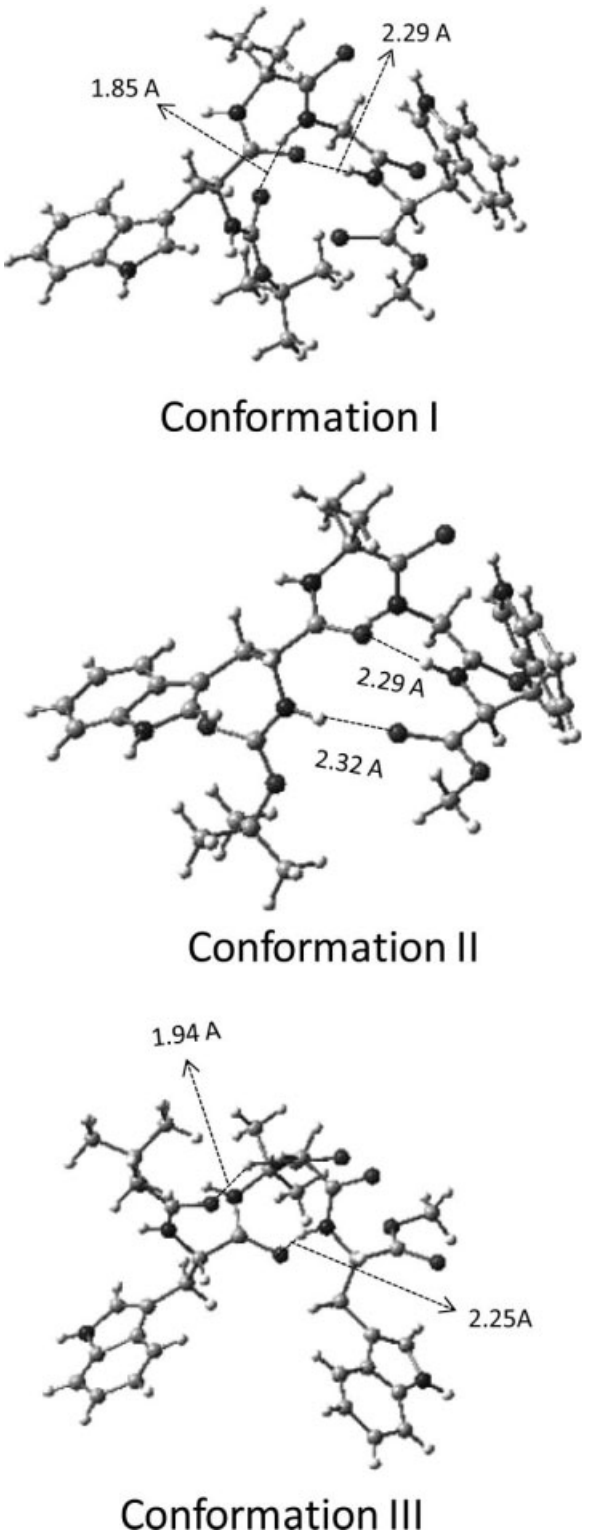

Fig. 1. Structures of initial, non-optimized conformations of WUGW-tetrapeptide (Conformations I, II, and III). Conformation I is taken from crystal structure (Ref. 50); Conformation II is derived from NMR data (Ref. 50); Conformation III has been built with backbone dihedral angles of 3_{10} helical structure.

another hydrogen bond (~2.32 Å) is between Trp_1 N—H and Trp_4 C=O. For Conformation III, one hydrogen bond (~2.25 Å) is between Trp_1 C=O and Trp_4 N—H, and another hydrogen bond (~1.94 Å) is between Boc-ester C=O and Gly_3 N—H.

The optimizations, in vacuum, of these three conformations at B3LYP/6-31G* level theory have led to their convergence into two structures that differ from each of the starting structures. The structural parameters of the fully optimized conformations are given in Table 2, while the structures themselves are displayed in Figure 2. Conformers I and II have converged into an intermediate structure (designated as Conformation A) with φ of Trp_1 residue as −75°. This dihedral angle is in between the angles of −55° and −150° for the starting Conformations I and II, respectively. Additionally, while the hydrogen bonds between Trp_1 C=O and Trp_4 N—H from conformers I and II, Trp_1 N—H and Trp_4 C=O from conformer II, Boc-ester C=O and Gly_3 N—H from conformer I are preserved in conformer A, an additional hydrogen bond (~2.41 Å), between Boc-ester C=O and Aib_2 N—H is present in conformer A. Conformation III has also been modified as a result of optimization into a structure designated as Conformation B. While one hydrogen bond between Boc-ester C=O and Gly_3 N—H (2.02 Å) present in Conformation B is preserved from Conformation III, a second hydrogen bond between Aib_2 C=O and Trp_4 N—H (2.17 Å) is newly formed as a result of optimization.

On the basis of the difference in predicted electronic energy values (ΔE = 6.12 kcal/mol), conformer A is significantly more stable than conformer B. Despite this large

TABLE 1. Backbone dihedral angles (degrees) in the three starting initial conformations[a] of Boc-Trp_1-Aib_2-Gly_3-Trp_4-OMe (WUGW) tetrapeptide

	φ	ψ[b]	ω[b]	χ_1[c]	χ_2[c]
Conformation I					
Trp_1	−55	131	177	−57	131
Aib_2	61	20	175		
Gly_3	94	4	179		
Trp_4	−155	−177	177	71	−74
Conformation II					
Trp_1	−150	131	177	−57	131
Aib_2	61	20	175		
Gly_3	94	4	179		
Trp_4	−155	−177	177	71	−74
Conformation III					
Trp_1	−61	−30	177	−57	131
Aib_2	−60	−31	175		
Gly_3	−61	−31	179		
Trp_4	−60	−30[a]	177[a]	178	−74

[a]Conformation I is taken from crystal structure (Ref. 50); Conformation II is taken from NMR structure (Ref. 50); Conformation III has been built with backbone dihedral angles of 3_{10} helical structure.

[b]Standard definitions of φ, ψ, and ω are used. For Trp_4, ψ and ω correspond to dihedral angles N−C−C−O(CH_3) and C−C−O−C(H_3), respectively.

[c]χ_1 and χ_2 correspond to dihedral angles N_{boc}−C−C−C(CN_{trp}) and (N_{boc}C)C−C−C−N_{trp}, respectively, for Trp_1 and N−C−C−C(CN_{trp}) and (NC)C−C−C−N_{trp}, respectively, for Trp_4.

TABLE 2. Backbone dihedral angles (degrees) in the two fully optimized conformations[a] of Boc-Trp_1-Aib_2-Gly_3-Trp_4-OMe (WUGW) tetrapeptide

	φ	ψ[b]	ω[b]	χ_1[c]	χ_2[c]
Conformation A					
Trp_1	−75	99	−168	−58	101
Aib_2	49	38	176		
Gly_3	106	−25	−162		
Trp_4	−134	179[a]	180[b]	61	−81
Conformation B					
Trp_1	−74	−13	169	−62	110
Aib_2	−52	−36	179		
Gly_3	−82	79	−172		
Trp_4	−147	−46[a]	−179[b]	−160	−108

[a]A is the converged conformation from initial structure of conformer I or II (Table 1). B is the converged conformation from initial structure of conformer III (Table 1).

[b]Standard definitions of φ, ψ, and ω are used. For Trp_4, ψ and ω correspond to dihedral angles $N-C-C-O(CH_3)$ and $C-C-O-C(H_3)$, respectively.

[c]χ_1 and χ_2 correspond to dihedral angles $N_{boc}-C-C-C(CN_{trp})$ and $(N_{boc}C)C-C-C-N_{trp}$, respectively, for Trp_1 and $N-C-C-C(CN_{trp})$ and $(NC)C-C-C-N_{trp}$, respectively, for Trp_4.

energy difference, both conformers have been subjected to VCD calculations to note the differences in theoretical spectra and evaluate the agreement with experimental spectra.

The comparison of experimental VA (bottom) and VCD (top) spectra obtained in $CHCl_3$ and CH_3OH solvents with the corresponding theoretical spectra of Conformations A and B is displayed in Figure 3. As can be seen from this figure, the dominant experimental VCD feature present in the amide I (C=O stretching) region is a negative band in both solvents (1666 cm^{-1} in $CHCl_3$ and 1655 cm^{-1} in CH_3OH). These negative VCD bands, for both solvents, are associated with the highest intensity absorption bands (1674 cm^{-1} in $CHCl_3$ and in CH_3OH 1666 cm^{-1}) in the region considered. A negative VCD band in the ~1648–1658 cm^{-1} range was also seen[2] in longer analogous-peptide sequences with β-hairpin (β-sheet + β-turn) structures in chloroform solvent. This negative band appears[2] (refer Fig. 3) at a slightly lower frequency (by about 10 cm^{-1}) in methanol solvent. Since the present tetrapeptide does not have a β-sheet structural component but also gives a negative VCD signal in the amide I region at ~1650–1660 cm^{-1}, this negative signal can be interpreted as originating from the β-turn structure.

For the predicted spectra, the turn structure represented by conformer A displays the characteristic features as a negative VCD signal at 1679 cm^{-1} and a positive VCD signal at 1730 cm^{-1}. The dominant negative VCD signal at 1679 cm^{-1} for Conformation A, correlates well in terms of position and intensity with the experimental negative VCD signals in both solvents. The predicted negative VCD signal originates from C=O stretching vibration of Trp_1 (refer Table 3), coupled to C=O stretching vibrations of Boc-ester, Aib_2 and Gly_3, with a scaled frequency of 1681 cm^{-1}. The intensity of this simulated negative VCD band is reduced by a neighboring vibration with positive VCD at a scaled frequency of 1691 cm^{-1}, which originates from C=O stretching vibration of Gly_3, coupled to C=O stretching vibrations of Trp_1 and Aib_2. The simulated positive VCD signal at ~1730 cm^{-1} of conformer A doesn't have a corresponding experimental band for correlation. This positive VCD signal originates from two vibrations with scaled frequencies of 1700 cm^{-1} and 1729 cm^{-1} (Table 3). The origin of the 1700 cm^{-1} vibration is C=O stretching vibration of Aib_2 with coupling to C=O stretching vibrations of Trp_1 and Gly_3. The origin of the 1729 cm^{-1} vibration is C=O stretching of Trp_4.

The turn structure represented by conformer B displays very weak VCD signals. The predicted VCD spectrum of Conformation B doesn't have any satisfactory agreement with the experimental spectra. The most noticeable negative VCD signal of conformer B is present at 1764 cm^{-1} and it originates from C=O stretching vibration of Trp_4 residue (Table 4). Even for a qualitative level comparison,

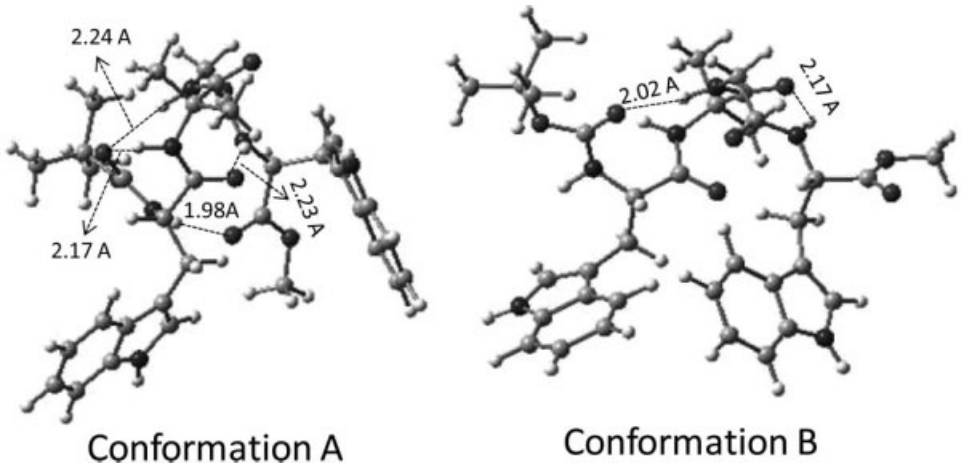

Fig. 2. Structures of fully optimized conformations of WUGW-tetrapeptide (Conformations A and B) using B3LYP functional and 6-31G* basis set. A is the converged conformation from initial structure of Conformer I or II (Fig. 1). B is the converged conformation from initial structure of Conformer III (Fig. 1).

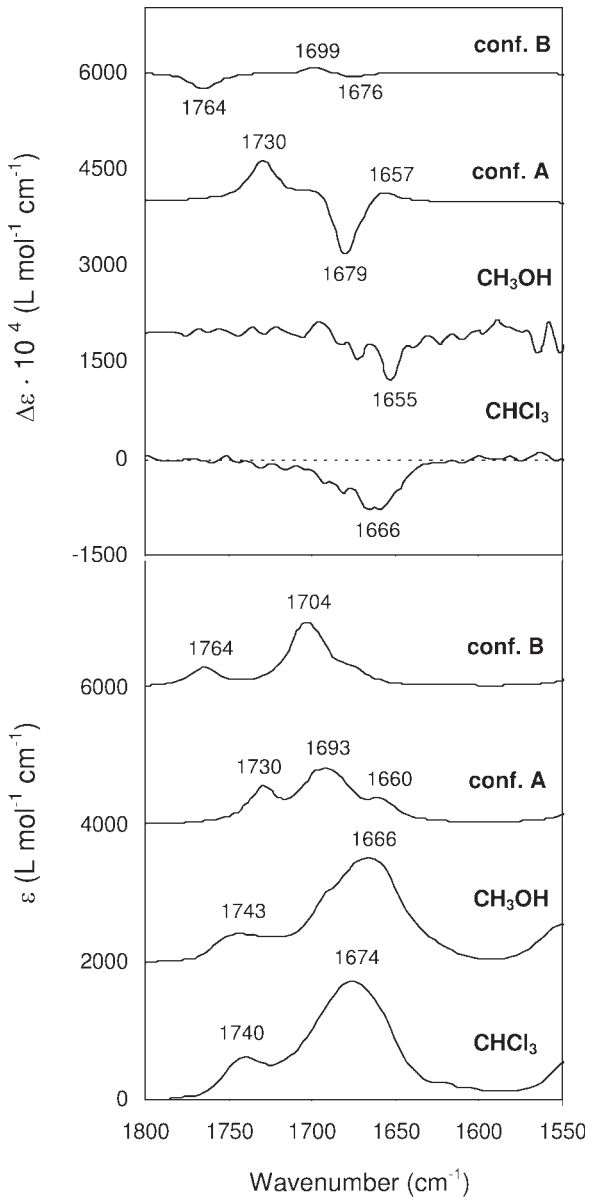

Fig. 3. Comparison of experimental and predicted vibrational absorption (lower panel) and VCD (upper panel) spectra. The predicted spectra are for the two converged optimized conformations (Conformations A and B) obtained using B3LYP functional and 6-31G* basis set.

this negative VCD signal is too far-removed to be correlated with the negative experimental signal.

Although positions of weaker VCD bands (positive band at 1657 cm^{-1} for Conformation A and negative couplet at 1699 and 1676 cm^{-1} for Conformation B) have been labeled in Figure 3, there are no corresponding experimental bands. The origins of these weaker predicted bands, nevertheless, have been identified based on data in Tables 3 and 4 as follows: the positive VCD signal at ~1657 cm^{-1} of Conformation A originates from C=O stretching vibration of Boc-ester with some coupling to C=O stretching vibration of Trp_1; the predicted negative VCD band at ~1676 cm^{-1} for conformer B originates from C=O stretching vibration of Aib_2 with coupling to C=O stretching vibrations of Trp_1 and Gly_3; the predicted positive VCD band at ~1699 cm^{-1} originates from three vibrations with scaled frequencies of 1696 cm^{-1}, 1704 cm^{-1}, and 1709 cm^{-1} (Table 4). Vibrations at 1696 cm^{-1} and 1704 cm^{-1} contribute to the intensity of the positive band, while vibration at 1709 cm^{-1} with negative rotational strength diminishes the positive VCD band intensity. The origin of the 1696 cm^{-1} is C=O stretching vibration of Trp_1 with coupling to the C=O stretching vibration of Aib_2. The origin of the 1704 cm^{-1} vibration is C=O stretching vibration of Gly_3 with coupling to the C=O stretching vibration of Boc-ester and Aib_2. The origin of the 1709 cm^{-1} vibration is C=O stretching vibration of Boc-ester with coupling to C=O stretching vibrations of Aib_2 and Gly_3.

It is disconcerting to note that the predicted VCD spectrum for conformer A has a positive VCD band at 1730 cm^{-1} with significant intensity for which no corresponding experimental band is seen. A possible explanation for this mismatch is that the calculations are done for isolated molecules, while the experimental data are obtained in solution phase. The NMR spectral data for WUGW suggested[50] the presence of two conformers in equilibrium, but the geometry optimizations of these two conformers in vacuum lead to a single conformer A. Then it is to be construed that the NMR data are indicating solvent mediated stability of conformers I and II, and therefore, VCD calculations have to be undertaken for these two conformers.

The solvent influence on geometry optimizations can be incorporated using approximate models such as polarizable continuum model (PCM),[60] but our attempts to optimize the current tetrapeptide geometries using PCM

TABLE 3. Predicted parameters associated with five vibrations giving rise to the dominant VCD signals of Conformation A

Simulated VCD bands (cm^{-1})	(+), 1657	(−), 1679		(+), 1730	
Unscaled freq. (cm^{-1})	1725	1749	1759	1769	1799
Scaled freq. (cm^{-1})	1659	1681	1691	1700	1729
Dipole strength (10^{-40} esu^2 cm^2)	470.73	476.91	636.96	679.52	777.64
Rotational strength (10^{-44} esu^2 cm^2)	110.23	−476.46	155.36	61.28	267.94
Carbonyl group			Relative displacement[a]		
Boc-ester	**1.0472**	−0.1516	0.0430	−0.0871	0.1022
Trp_1	0.1734	**0.9881**	−0.1733	0.3233	−0.0056
Aib_2	0.0277	−0.2971	0.1926	**1.0717**	0.0297
Gly_3	−0.0138	0.2119	**1.1165**	−0.1269	−0.1045
Trp_4	0.0874	−0.0457	−0.1004	0.0351	**−1.1764**

[a]The relative displacements are listed for carbonyl groups belonging to Boc, Trp_1, Aib_2, Gly_3, and Trp_4 residue to identify which residue(s) has the most pronounced C=O stretching for a given predicted vibration.

TABLE 4. Predicted parameters associated with five vibrations giving rise to the dominant VCD signals of Conformation B

Simulated VCD bands (cm^{-1})	(−), 1676		(+), 1699		(−), 1764
Unscaled freq. (cm^{-1})	1743	1765	1773	1777	1836
Scaled freq. (cm^{-1})	1676	1696	1704	1709	1765
Dipole strength (10^{-40} esu^2 cm^2)	282.44	607.07	754.22	433.09	425.81
Rotational strength (10^{-44} esu^2 cm^2)	−37.64	22.45	40.71	−32.15	−108.87
Carbonyl group			Relative displacement[a]		
Boc-ester	0.1117	0.0441	0.4491	**0.9991**	−0.0075
Trp_1	−0.1975	**1.1394**	0.0459	−0.0481	−0.0192
Aib_2	**1.1108**	0.1657	0.1394	−0.1922	−0.0091
Gly_3	0.2038	0.0961	**−0.9815**	0.4263	0.0000
Trp_4	0.0079	0.0200	0.0087	0.0079	**1.2649**

[a]The relative displacements are listed for carbonyl groups belonging to Boc, Trp_1, Aib_2, Gly_3, and Trp_4 residue to identify which residue(s) has the most pronounced C=O stretching for a given predicted vibration.

model turned out to be unsuccessful. Explicit inclusion of solvent molecules[61] is one way to overcome this problem, but such calculations increase the number of basis functions leading to computational limitations.

We have also undertaken the VCD calculations at the geometries of conformers I and II, as obtained from crystal structure and NMR data, without any geometry optimization, but this procedure led to unrealistic vibrational mode descriptions. This is because, bond lengths and angles obtained from the crystal structure and NMR data are often significantly different from those in optimized geometries. For example, C=O bond lengths in crystal structure are ~1.5 A, which are more like single bond lengths and, as a result, the predicted carbonyl stretching vibrations appeared at much lower frequencies mixed with C—C and C—N stretching vibrations.

To overcome these problems, we chose to fix the backbone dihedral angle values of φ, ψ, and ω in conformers I and II to those found in crystal and NMR data and optimize the bond lengths and angles. Such constrained optimization resulted in realistic bond lengths and angles while preserving the turn geometries found in crystal and NMR data. The constrained optimization was allowed for 65 cycles of optimization. Although conformers I and II with constrained optimization were not found to be at the potential energy minimum (as indicated by one imaginary vibrational frequency), this can be expected as the solvent mediated stability is not built into the calculation. Nevertheless, the vibrational spectra predicted for these conformers may be expected to capture the dominant features that would have been obtained by including explicit solvent influence.

Comparison of the experimental spectra with those predicted for constraints-imposed partially optimized Conformations I and II is presented in Figure 4. The predicted VCD spectra now display one predominant negative VCD band which corresponds to the negative experimental VCD band observed in solution. Specifically, the experimental negative VCD band at ~1650 cm^{-1} arising from the highest intensity absorption band seems to correspond to the predicted negative VCD band (at 1689 cm^{-1} for conformer I and 1684 cm^{-1} for conformer II) also arising from the highest intensity absorption bands. Although there are also weak positive VCD bands in the predicted spectra

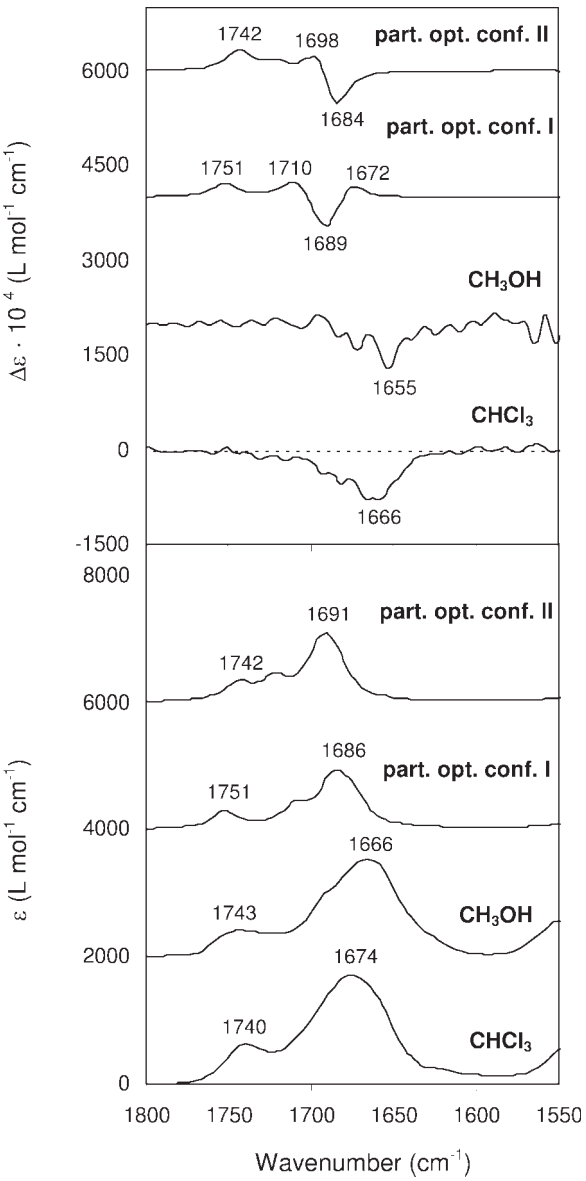

Fig. 4. Comparison of experimental and predicted vibrational absorption (lower panel) and VCD (upper panel) spectra. The predicted spectra are for the two constraints-imposed partially optimized β-turn conformations (Conformations I and II) obtained using B3LYP functional and 6-31G* basis set.

TABLE 5. Predicted parameters associated with vibrations giving rise to the VCD signals of constraints-imposed optimized Conformation I

Simulated VCD bands (cm^{-1})	(+), 1672	(−), 1689		(+), 1710	(+), 1751
Unscaled freq. (cm^{-1})	1743	1753	1758	1778	1823
Scaled freq. (cm^{-1})	1675	1685	1690	1710	1752
Dipole strength (10^{-40} esu^2 cm^2)	679.66	769.46	464.22	488.74	425.27
Rotational strength (10^{-44} esu^2 cm^2)	110.60	64.15	−299.30	133.65	85.55
Carbonyl group			Relative displacement[a]		
Boc-ester	−0.3931	**−0.9904**	0.3777	−0.1760	−0.0371
Trp1	0.0699	0.1061	−0.2020	**−1.0770**	0.1336
Aib2	**−1.0506**	0.4049	−0.1456	−0.0074	0.0000
Gly3	−0.0127	−0.4316	**−1.0889**	0.1476	0.0871
Trp4	−0.0313	−0.0095	0.1238	0.1035	**1.2681**

[a]The relative displacements are listed for different vibrations to identify which group(s) exhibits the most pronounced stretching.

they are not the dominant ones. Since both constraints-imposed partially optimized Conformations I and II are predicted to have a dominant negative VCD signal, as found in the experimental VCD spectra, one can surmise that both Conformations I and II might be present in solution, as deduced from the NMR study.[50]

The origins of the predicted bands for constraints-imposed partially optimized Conformations I and II are provided in Tables 5 and 6, respectively. The correlated negative band at ~1689 cm^{-1} of constraints-imposed optimized Conformation I originates from two vibrations with scaled frequencies of 1685 cm^{-1} and 1690 cm^{-1}. Vibration at 1685 cm^{-1} with positive rotational strength diminishes the intensity of vibration at 1690 cm^{-1} with negative rotational strength. The origin of 1685 cm^{-1} vibration is the C=O stretching of Boc-ester with coupling to C=O stretching vibration of Aib_2 and Gly_3. The origin of the 1690 cm^{-1} vibration is the C=O stretching of Gly_3 with coupling to C=O stretching vibrations of Boc-ester and Trp_1. In terms of the correlated negative VCD band at ~1684 cm^{-1} of constraints-imposed optimized Conformation II, it originates from C=O stretching vibration of Trp_1 with coupling to C=O stretching vibrations of Boc-ester, Aib_2 and Gly_3.

The results presented in the previous paragraphs suggest that both Type II–I′ β-turn (conformer I) and Type I′ β-turn (conformer II) yield a negative amide I VCD signal as the dominant feature. A negative VCD, followed by positive VCD at a much higher frequency, are predicted for a structure intermediate (conformer A) between conformers I and II. Since the experimental VCD spectra for WUGW peptide show a single dominant negative amide I VCD band, the presence of conformers I and II for WUGW peptide is implicated, in agreement with the predictions[50] from NMR data.

For general conclusions regarding what type of VCD signals may be associated with β-turn geometries, it is to be noted that the current WUGW-tetrapeptide is known[50] to exist in equilibrium between two Type I′ turn structures (conformers I and II). The experimental VCD spectrum of this tetra peptide exhibits a dominant negative VCD band in the 1670–1650 cm^{-1} region. Quantum chemical predictions of VCD for conformers I and II, do yield a dominant negative VCD signal (Fig. 4) that correlates with the experimental VCD band. Thus, it appears that typical Type I′ turns can be associated with one dominant negative VCD band at about 1650 cm^{-1}. However, some variations to this generalization can be expected depending on the composition of residues and the distortion of angles in Type I′ turn. Conformer A, representing a distorted Type I′ turn, where the angles for $i+1$ and $i+2$ residues differed from standard turn angles by up to ~25°, yielded a significant positive VCD band on the higher wavenumber side of the negative VCD band. A predominantly negative VCD band, with a weak positive shoulder on the higher wavenumber side, was also predicted[49] for Type I′ turn in Ac-Ala-Ala-NMe.

TABLE 6. Predicted parameters associated with vibrations giving rise to the VCD signals of constraints-imposed optimized Conformation II

Simulated VCD bands (cm^{-1})	(−), 1684	(+), 1698		(+), 1742	
Unscaled freq. (cm^{-1})	1754	1761	1766	1791	1814
Scaled freq. (cm^{-1})	1686	1693	1697	1722	1744
Dipole strength (10^{-40} esu^2 cm^2)	899.58	654.91	527.49	494.40	429.81
Rotational strength (10^{-44} esu^2 cm^2)	−374.70	217.68	64.08	48.76	122.77
Carbonyl group			Relative displacement[a]		
Boc-ester	0.1953	0.0678	0.0286	**1.1477**	−0.1689
Trp1	**−1.0248**	−0.2275	−0.3562	0.2202	0.0904
Aib2	0.2321	**−1.1314**	0.0570	0.0287	−0.0191
Gly3	−0.3391	−0.0187	**1.1368**	0.0469	0.1109
Trp4	0.1445	0.0091	−0.0844	0.1445	**1.2450**

[a]The relative displacements are listed for different vibrations to identify which group(s) exhibits the most pronounced stretching.

Thus it appears that although Type I′ turn can be associated with a dominant negative VCD band at about 1650 cm^{-1}, sometimes an additional positive VCD band on the higher wavenumber side cannot be ruled out. Synthesis of, and VCD investigations on, additional small peptides containing turn structure as the sole structural motif are expected to be useful for expanding on these conclusions.

CONCLUSIONS

The first comparison of experimental VCD spectra with corresponding fully quantum chemical (both optimization and VCD) predictions has been performed for a β-turn-forming WUGW-tetrapeptide. This report additionally establishes the vibrational origins of the bands in all of the predicted VCD spectra for the tetrapeptide under investigation. The predicted VCD spectrum of fully optimized Conformation A results in the reproduction of the dominant negative VCD signal observed experimentally, but exhibits an extra positive band which is not seen in the experimental spectrum. This mismatch could be resulting from the lack of solvent influence in the quantum chemical geometry optimizations. However, Conformations I and II, which mimic the solvent stabilized structures, are predicted to have dominant negative VCD bands as found in the experimental spectra, indicating that both conformations might be present in solution. On the basis of the observations for WUGW-tetrapeptide, it is noted that quantum chemical geometry optimizations for peptides with β-turn propensity in vacuum are not advisable since they are likely to converge to structures that are not the realistic models of conformations found in solution. It is also not advisable to do quantum chemical vibrational property calculations directly on geometries obtained from crystal data or NMR data, as they result in unrealistic vibrational frequencies and descriptions. In the absence of explicit solvent influence on calculated geometries, constraining the backbone dihedral angles to those found in condensed medium, and optimizing the remaining geometrical parameters appears to provide satisfactory vibrational properties for β-turn-forming peptides in the condensed medium.

ACKNOWLEDGMENT

Computational work utilized the NCSA IBM P690 and SGI Altix systems. Teaching assistantship from Vanderbilt University (to A.G.P.) is greatly appreciated. R.M. was supported by the award of a Senior Research Fellowship from the Council of Scientific and Industrial Research, India.

LITERATURE CITED

1. Zhao C, Polavarapu PL, Das C, Balaram P. Vibrational circular dichroism of beta-hairpin peptides. J Am Chem Soc 2000;122:8228–8231.
2. Mahalakshmi R, Shanmugam G, Polavarapu PL, Balaram P. Circular dichroism of designed peptide helices and beta-hairpins: analysis of Trp- and Tyr-Rich peptides. Chem Biol Chem 2005;6:2152–2158.
3. Krittanai C, Johnson WC. Correcting the circular dichroism spectra of peptides for contributions of absorbing side chains. Anal Biochem 1997;253:57–64.
4. Lal BB, Nafie LA. Vibrational circular dichroism in amino acids and peptides. 7. Amide stretching vibrations in polypeptides. Biopolymers 1982;21:2161–2183.
5. Sen AC, Keiderling TA. Vibrational circular dichroism of polypeptides. III. Film studies of several alpha-helical and beta-sheet polypeptides. Biopolymers 1984;23:1533–1545.
6. Lipp ED, Nafie LA. Vibrational circular dichroism in amino acids and peptides. 10. Fourier transform VCD and Fourier self-deconvolution of the amide I region of poly(gamma-benzyl-L-glutamate). Biopolymers 1985;24:799–812.
7. Yasui SC, Keiderling TA, Bonora GM, Toniolo C. Vibrational circular dichroism of polypeptides, V. A study of 3_{10}-helical-octapeptides. Biopolymers 1986;25:79–89.
8. Yasui SC, Keiderling TA. Vibrational circular dichroism of polypeptides. VI. Polytyrosine alpha-helical and random-coil results. Biopolymers 1986;25:5–15.
9. Narayanan U, Keiderling TA, Bonora GM, Toniolo C. Vibrational circular dichroism of polypeptides. 7. Film and solution studies of beta-sheet-forming homooligopeptides. J Am Chem Soc 1986;108:2431–2437.
10. Pancoska P, Yasui SC, Keiderling TA. Enhanced sensitivity to conformation in various proteins. Vibrational circular dichroism results. Biochemistry 1989;28:5917–5923.
11. Pancoska P, Wang L, Keiderling TA. Frequency analysis of infrared absorption and vibrational circular dichroism of proteins in D_2O solution. Protein Sci 1993;2:411–419.
12. Nafie LA, Freedman TB. Vibrational circular dichroism: An incisive tool for stereochemical applications. Enantiomer 1998;3:283–297.
13. Zhao C, Polavarapu PL. Vibrational circular dichroism of gramicidin in organic solvents. Biospectroscopy 1999;5:276–283.
14. Zhao C, Polavarapu PL. Vibrational circular dichroism is an incissive structural probe: ion induced structural changes in gramicidin D. J Am Chem Soc 1999;121:11259–11260.
15. Zhao C, Polavarapu PL. Vibrational circular dichroism of Gramicidin D in vesicles and micelles. Biopolymers (Biospectroscopy) 2001; 62:336–340.
16. Keiderling TA. Protein and peptide secondary structure and conformational determination with vibrational circular dichroism. Curr Opion Chem Biol 2002;6:682–688.
17. Boricks A, Murphy RF, Lovas S. Fourier transform vibrational circular dichroism as a decisive tool for conformational studies of peptides containing tyrosyl residues. Biopolymers (Biospectroscopy) 2003; 72:21–24.
18. Mazaleyrat JP, Wright K, Gaucher A, Toulemonde N, Wakselman M, Oancea S, Peggion C, Formaggio F, Setnicka V, Keiderling TA, Toniolo C. Induced axial chirality in the biphenyl core of the Cα-tetrasubstituted α-amino acid residue Bip and subsequent propagation of chirality in (Bip)n/Val oligopeptides. J Am Chem Soc 2004;126: 12874–12879.
19. Taniguchi T, Miura N, Nishimura S, Monde K. Vibrational circular dichroism; Chiroptical analysis of biomolecules. Mol Nutr Food Res 2004;48:262–254.
20. Xie P, Zhou Q, Diem M. Conformational studies of beta-turns in cyclic-peptides by vibrational circular dichroism. J Am Chem Soc 1995;117:9502–9508.
21. Gulotta M, Goss DJ, Diem M. IR vibrational CD in model deoxyoligonucleotides: observation of the B-Z phase transition and extended coupled oscillator intensity calculations. Biopolymers 1989;28:2047–2058.
22. Xiang T, Goss DJ, Diem M. Strategies for the computation of infrared CD and absorption spectra of biological molecules: ribonucleic acids. Biophys J 1993;65:1255–1261.
23. Bour P, Keiderling TA. Ab initio simulations of the vibrational circular dichroism of coupled peptides. J Am Chem Soc 1993;115:9602–9607.
24. Bour P, Sopkova J, Bednarova L, Malon P, Keiderling TA. Transfer of molecular property tensors in cartesian coordinates: a new algorithm for simulation of vibrational spectra. J Comput Chem 1997;18:646–659.

25. Bour P, Kubelka J, Keiderling TA. Simulations of oligopeptide vibrational CD: effects of isotopic labeling. Biopolymers 2000;53:380–395.
26. Silva RAGD, Kubelka J, Bour P, Decatur SM, Keiderling TA. Site-specific conformational determination in thermal unfolding studies of helical peptides using vibrational circular dichroism with isotopic substitution. Proc Natl Acad Sci USA 2000;97:8318–8323.
27. Kubelka J, Kiderling TA. The anomalous infrared amide I intensity distribution in 13C isotopically labeled peptide β-sheets comes from extended, multiple-stranded structures. An ab initio study. J Am Chem Soc 2001;123:6142–6150.
28. Kubelka J, Kiderling TA. Differentiation of β-sheet-forming structures: ab initio-based simulations of IR absorption and vibrational CD for model peptide and protein β-sheets. J Am Chem Soc 2001;123:12048–12058.
29. Hilario J, Kubelka J, Syud FA, Gellman SH, Keiderling TA. Spectroscopic characterization of selected beta-sheet hairpin models. Biopolymers (Biospectroscopy) 2002;67:233–236.
30. Bour P, Keiderling TA. Vibrational spectral simulation for peptides of mixed secondary structure: method comparisons with the trpzip model hairpin. J Phys Chem B 2005;109:23687–23697.
31. Kim J, Huang R, Kubelka J, Bour P, Keiderling TA. Simulation of infrared spectra for beta-hairpin peptides stabilized by an aib-gly turn sequence: correlation between conformational fluctuation and vibrational coupling. J Phys Chem B 2006;110:23590–23602.
32. King WT, Zelano AJ. Sum rule for molecular frequencies. J Chem Phys 1967;47:3197–3198.
33. Polavarapu PL. A sum rule for vibrational circular dichroism intensities of fundamental transitions. J Chem Phys 1986;84:542–543.
34. Polavarapu PL. An approximate relation for paramagnetic magnetizability emerging from the sum rules for cartesian magnetic dipole moment derivatives. Chem Phys Lett 1990;171:271–276.
35. Polavarapu PL. Sum rules for cartesian polarizability derivative tensors. Chem Phys Lett 1990;174:511–516.
36. Bour P, Kubelka J, Keiderling TA. Ab initio quantum mechanical models of peptide helices and their vibrational spectra. Biopolymers 2002; 65:45–59.
37. Cheeseman J. Calculation of molecular chiroptical properties using density functional theory. ACS national meeting, Chicago, IL: 2007.
38. Bour P, Keiderling TA. Structure, spectra and the effects of twisting of β-sheet peptides. A density functional theory study. J Mol Struct (Theochem) 2004;675:95–105.
39. Bodack LA, Freedman TB, Chowdhry BZ, Nafie LA. Solution conformations of cyclosporins and magnesium-cyclosporin complexes determined by vibration circular dichroism. Biopolymers 2004;73:163–177.
40. Vass E, Hollosi M, Besson F, Buchet R. Vibrational spectroscopic detection of beta- and gamma-turns in synthetic and natural peptides and proteins. Chem Soc Rev 2003;103:1917–1954.
41. Stotz CE, Topp EM. Applications of model β-hairpin peptides. J Pharm Sci 2004;93:2881–2894.
42. Csaszar AG, Perczel A. Ab initio characterization of building units in peptides and proteins. Prog Biophys Mol Biol 1999;71:243–309.
43. Rose GD, Geirasch LM, Smith JA. Adv Prot Chem 1985;37:1–109.
44. Polavarapu PL, Zhao C. Vibrational circular dichroism: a new structural tool for biomolecular structural determination. Fresenius J Anal Chem 2000;366:727–734.
45. Xie P, Zhou Q, Diem M. IR circular dichroism of turns in small peptides. Faraday Discuss 1994;99:233–243.
46. Wyssbrod HR, Diem M. IR (vibrational) CD of peptide -turns: a theoretical and experimental study of cyclo-(-Gly-Pro-Gly-D-Ala-Pro-). Biopolymers 1992;32:1237–1242.
47. Hilario J, Kubelka J, Keiderling TA. Optical spectroscopic investigations of model β-sheet hairpins in aqueous solution. J Am Chem Soc 2003;125:7562–7574.
48. Xie P, Diem M. Conformational studies of cyclo-(-Pro-Gly-)$_3$ and its complexes with cations by vibrational circular dichroism. J Am Chem Soc 1995;117:429–437.
49. Kim J, Kapitan J, Lakhani A, Bour P, Keiderling TA. Tight beta turns in peptides. DFT-based study of infrared absorption and vibrational circular dichroism for various conformers including solvent effects. Theor Chem Acc 2008;119:81–97.
50. Mahalakshmi R, Sengupta A, Raghothama S, Shamala N, Balaram P. Tryptophan rich peptides: influence of indole rings on backbone conformation. Pept Sci 2006;88:36–54.
51. Aravinda S, Shamala N, Das C, Sriranjini A, Karle IL, Balaram P. Aromatic–aromatic interactions in crystal structures of helical peptide scaffolds containing projecting phenylalanine residues. J Am Chem Soc 2003;125:5308–5315.
52. Mahalakshmi R, Raghothama S, Balaram P. NMR analysis of aromatic interactions in designed peptide β-hairpins. J Am Chem Soc 2006; 128:1125–1138.
53. Aravinda S, Shamala N, Roy RS, Balaram P. Non-protein amino acids in peptide design. Proc Indian Acad Sci (Chem Sci) 2003;115:373–400.
54. Venkatraman J, Shankaramma SC, Balaram P. Design of folded peptides. Chem Rev 2001;101: 3131–3152.
55. Shanmugam G, Polavarapu PL. Vibrational circular dichroism of protein films. J Am Chem Soc 2004;126:10292–10295.
56. Karle IL, Balaram P. Structural characteristics of alpha-helical peptide molecules containing Aib residues. Biochemistry 1990;29:6747–6756.
57. Toniolo C, Crisma M, Bonora GM, Benedetti E, Blasio DB, Pavone P, Pedine C, Santini A. Preferred conformation of the terminally blocked (Aib)10 homo-oligopeptide: a long, regular 3_{10}-helix. Biopolymers 1991;31:129–138.
58. Karle IL, Flippen- Anderson JL, Gurunath R, Balaram P. Facile transition between 310- and alpha-helix: structures of 8-, 9-, and 10-residue peptides containing the -(Leu-Aib-Ala)2-Phe-Aib- fragment. Protein Sci 1994;3:1547–1555.
59. Mammi S, Rainaldi M, Bellanda M, Schievano E, Peggion E, Broxterman QB, Formaggio F, Crisma M, Toniolo C. Concomitant occurrence of peptide 310- and α-helices probed by NMR. J Am Chem Soc 2000;122:11735–11736.
60. Tomasi J, Cammi R, Mennucci B. Medium effects on the properties of chemical systems: an overview of recent formulations in the polarizable continuum model (PCM). Int J Quantum Chem 1999;75:783–803.
61. Zhang P, Polavarapu PL. Spectroscopic investigation of the structures of dialkyl tartrates and their cyclodextrin complexes. J Phys Chem A 2007;111:858–871.